JOURNAL OF Materials CHEMISTRY

Discotic liquid crystals of transition metal complexes 27:† supramolecular structure of liquid crystalline octakis-alkylthiophthalocyanines and their copper complexes

Kazue Ban, Kaoru Nishizawa, Kazuchika Ohta* and Hirofusa Shirai

Department of Functional Polymer Science, Faculty of Textile Science and Technology, Shinshu University, 386-8567 Ueda, Japan. E-mail: ko52517@giptc.shinshu-u.ac.jp

Received 4th January 2000, Accepted 10th February 2000
Published on the Web 30th March 2000

A series of octakisalkylthiophthalocyanines, $(C_nS)_8PcH_2$ ($n=8$, 10, 12, 16), and their copper(II) complexes, $(C_nS)_8PcCu$ ($n=8$, 10, 12, 16), have been synthesized. Their mesomorphism and supramolecular structures have been investigated by using differential scanning calorimetry, polarizing microscopy, temperature-dependent X-ray diffraction technique and temperature-dependent electronic spectroscopy. From the X-ray diffraction and electronic spectral results, it was revealed that each of the compounds has a D_h mesophase in which columnar structures the molecules form a mixture of the parts of aggregated dimers and monomers. The shapes of dimers are discussed by exciton coupling theory (Kasha's rule).

1 Introduction

Phthalocyanine is a π-conjugated macrocycle with the ability to coordinate with various metal ions. Their unique properties such as semiconductivity, electroconductivity, photoconductivity and non-linear optics have been widely studied for both fundamental science and application as optomagnetically recording materials.[2] Phthalocyanine-based discotic liquid crystals can be expected to find application as conducting devices, because they have self-assembling supramolecular structures. Schouten *et al.* reported an interesting relationship between discotic mesomorphism and the electroconductivities of the octakis(alkoxy) substituted phthalocyanines (abbreviated as $(C_nO)_8PcH_2$ hereafter).[3] These alkoxy-substituted phthalocyanines[4] show a blue-shift of the Q bands in the electronic absorption spectra, compared with that of alkyl-substituted core phthalocyanine.[5] This is attributable to the greater electron-donating ability of the alkoxy chains than the alkyl chains.

Hence, we inferred from Hammett's σ_p values (Table 1) that if the phthalocyanine were substituted by eight non-electron-donating alkylthio groups instead of alkyl groups, the Q band would red-shift, compared with the alkoxy-substituted phthalocyanines. The red-shift of the Q band means that the band gap between the HOMO and the LUMO becomes smaller on introduction of the alkylthio substituents, because the Q band corresponds to the HOMO–LUMO transition. Accordingly, the electroconductivity may increase. Adam *et al.* reported that a discotic liquid crystal of triphenylene substituted by alkylthio groups exhibits considerably higher charge carrier mobility in the discotic mesophase, compared with conventional organic semiconductors.[6] It can be inferred from this example that sulfur atoms may significantly influence the conductivity of the mesophase. While we were carrying out this study, Eichhorn and Wöhrle reported the first example of the columnar mesomorphism of octakis(octylthio)-substituted phthalocyanine and the zinc and copper complexes.[7] In the present study, we have synthesized a series of octakis-(alkylthio)-phthalocyanines (abbreviated as $(C_nS)_8PcH_2$, $n=8$, 10, 12, 16) and their copper complexes (abbreviated as $(C_nS)_8PcCu$, $n=8$, 10, 12, 16), and thoroughly investigated their mesomorphism. In this paper, we will discuss the influence of sulfur atoms and the chain length on the mesomorphism and unique aggregated dimer structures in the columnar mesophase.

†For part 26, see ref. 1.

Table 1 Hammett's σ_p values[a]

Substituent	CH_3O-	CH_3-	H-	CH_3S-
σ_p	−0.27	−0.17	0	0

[a]These values are taken from ref. 15.

2 Experimental

2-1 Measurements

The products synthesized here were identified by ^{1}H-NMR (JEOL JNM-FX90A) and IR (Jasco A-100). Further identifications of the phthalocyanine derivatives were made by elemental analysis (Perkin-Elmer elemental analyzer 2400) and electronic absorption spectroscopy (Hitachi 330 spectrophotometer).

The phase transition behaviors of these compounds were observed by using a polarizing microscope (Olympus BH2), equipped with a heating plate controlled by a thermoregulator (Mettler FP80 hot stage, Mettler FP82 Central Processor), and measured by a differential scanning calorimeter (Shimadzu DSC-50). The X-ray diffraction measurements were performed with Cu-Kα radiation (Rigaku Geigerflex and Rigaku Rint) equipped with a hand-made heating plate[8] controlled by a thermoregulator. Temperature-dependent electronic absorption spectra were measured by a Hitachi 330 spectrophotometer equipped with a hand-made heating plate[9] controlled by a thermoregulator for films of the phthalocyanine derivatives. These thin films were prepared by casting from chloroform solution on P102 glass.

2-2 Synthesis

The synthetic route is shown in Scheme 1. The synthesis of 4,5-bis(alkylthio)phthalonitrile was carried out at first by the method of Suda *et al.*,[10] but the target compound could not be obtained. Hence, we adopted the method of Wöhrle *et al.*[11] The syntheses of octakis(alkylthio)phthalocyanine and octakis-

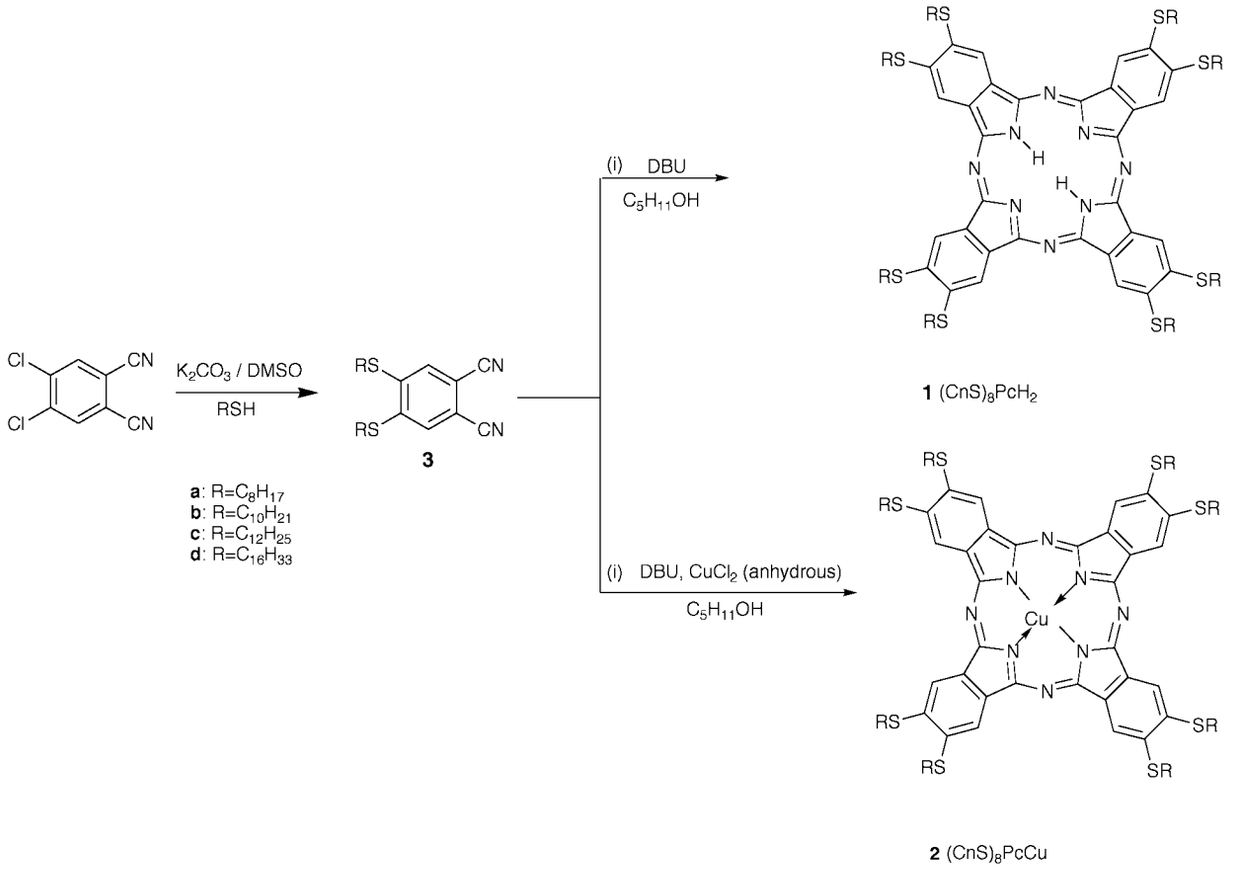

Scheme 1 Synthetic route to the octakis(alkylthio)phthalocyanine derivatives; **1a**, **1b**, **1c** and **1d**, and the corresponding copper(II) complexes; **2a**, **2b**, **2c** and **2d**. DBU = 1,8-diazabicyclo[5.4.0]undec-7-ene. (i) See refs. 7 and 11.

(alkylthio)phthalocyaninatocopper(II) also were carried out by the method of Wöhrle *et al.*[7,11] The detailed procedures for the representative compounds, $(C_8S)_8PcH_2$ **1a** and $(C_8S)_8PcCu$ **2a**, are described in the following.

4,5-Bis(octylthio)phthalonitrile (3a). A mixture of octane-1-thiol (1.78 g, 12.2 mmol) and 4,5-dichlorophthalonitrile (1.00 g, 5.08 mmol) in dry DMSO was heated up to 100 °C with stirring under a nitrogen atmosphere. Dry finely powdered K_2CO_3 was added (5 × 1.40 g, one portion every 5 min). Then, the mixture was stirred at 100 °C for 30 min. After cooling to room temperature, it was diluted with chloroform. The organic layer was washed with water and dried over Mg_2SO_4. After removal of the solvent, purification was carried out by recrystallization twice from *n*-hexane to give 1.31 g of white solid. Yield 62%. Mp = 58.8–59.0 °C.

^{1}H-NMR ($CDCl_3$, TMS) δ 0.90 (t, J = 5.7 Hz, 6H, CH_3), 1.82–1.31 (m, 24H, CH_2), 3.02 (t, J = 7 Hz, 4H, -CH_2-S-), 7.41–7.26 (m, 2H, Ph).

IR (KBr) ν_{max} 2900 (CH_2), 2250 cm^{-1} (-CN).

Octakis(octylthio)phthalocyanine (1a). Compound **3a** (0.30 g, 0.72 mmol) in pentan-1-ol (10 ml) was refluxed in the presence of 1,8-diazabicyclo[5.4.0]undec-7-ene (DBU) (0.22 g, 1.45 mmol) with stirring for 20.5 hours. After cooling to room temperature, pentan-1-ol was distilled off under reduced pressure. Purification was carried out by column chromatography (silica gel, chloroform, R_f = 1.00) and then the solvent was removed. The residue was washed with methanol several times and then recrystallized from a mixture of ethyl acetate and pentan-2-ol (2 : 1), to afford 0.11 g of green solid. Yield 37%.

^{1}H-NMR ($CDCl_3$, TMS) δ −3.24 (br s, 2H, -NH-), 0.91 (t, J = 7.02 Hz, 24H, CH_3), 1.78–1.36 (m, 80H, CH_2), 2.08–2.06 (m, 16H, CH_2), 3.44 (t, J = 7 Hz, 16H, -CH_2-S-), 8.48 (s, 8H, Ph).

IR (KBr) ν_{max} 2930, 2850 (CH_2), 1590 (Ph), 750 cm^{-1} (S-CH_2).

Octakis(octylthio)phthalocyaninatocopper(II) (2a). A mixture of compound **3a** (1.00 g, 2.40 mmol), copper(II) chloride

Table 2 Elemental analysis data, recrystallization solvents and yields of the $(C_nS)_8PcM$ (M = 2H, Cu; n = 8, 10, 12, 16) derivatives

	Elemental analysis; Found (%) (Calcd. %)						
Compound	C	H	N	S	Recrystallization solvent	Yield (%)	Virgin state
1a: $(C_8S)_8PcH_2$	68.72 (69.10)	8.68 (8.82)	6.72 (6.72)	15.66 (15.37)	AcOEt + $(CH_3)_2CHOH$	56	K
1b: $(C_{10}S)_8PcH_2$	71.15 (71.06)	9.52 (9.48)	5.96 (5.92)	13.85 (13.55)	AcOEt	49	K_4
1c: $(C_{12}S)_8PcH_2$	72.37 (72.60)	9.89 (10.00)	5.34 (5.29)	11.90 (12.11)	AcOEt	54	K_2
1d: $(C_{16}S)_8PcH_2$	74.62 (74.88)	10.26 (10.76)	4.67 (4.37)	10.30 (10.00)	AcOEt	58	K_2
2a: $(C_8S)_8PcCu$	66.87 (66.64)	8.35 (8.39)	6.86 (6.48)	14.86 (14.83)	AcOEt + CH_2Cl_2	75	K
2b: $(C_{10}S)_8PcCu$	68.64 (68.82)	9.30 (9.08)	5.70 (5.73)		AcOEt + CH_2Cl_2	52	K
2c: $(C_{12}S)_8PCu$	71.06 (70.55)	9.54 (9.62)	5.30 (5.14)	11.07 (11.77)	AcOEt + CH_2Cl_2	69	K_1
2d: $(C_{16}S)_8PcCu$	72.87 (73.13)	10.13 (10.43)	4.49 (4.26)	9.57 (9.76)	AcOEt	83	$K_2 + K_3 + K_4 + K_5$

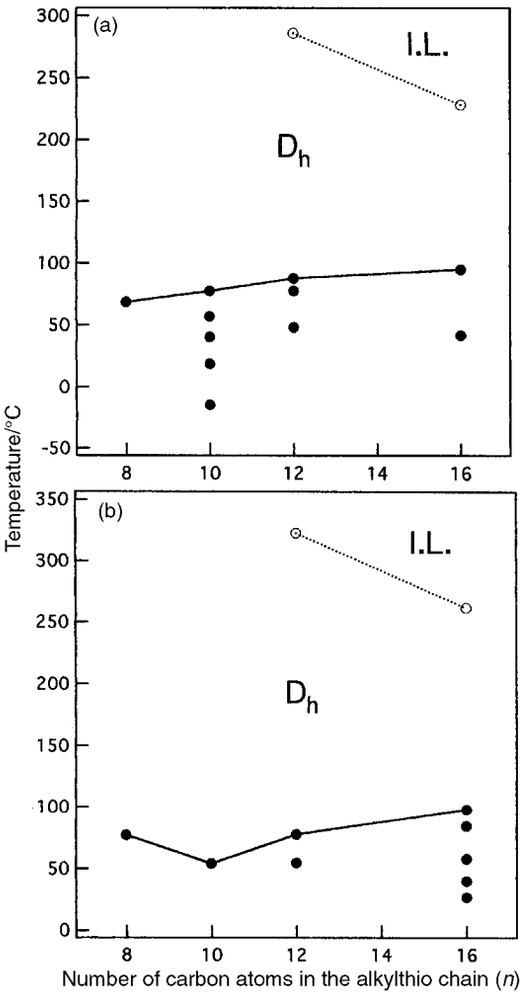

Fig. 1 Phase transition temperatures of (a) $(C_nS)_8PcH$ and (b) $(C_nS)_8PcCu$. The filled circles and open circles mean melting points and clearing points, respectively.

(anhydrous, 0.08 g, 0.60 mmol), and DBU (0.47 g, 3.09 mmol) in pentan-1-ol (25 ml) was refluxed for 25 hours. The reaction mixture was cooled and separated by filtration. The remaining precipitate was washed with methanol. The residue was purified by column chromatography (silica gel, benzene, $R_f = 1.00$) and recrystallized from ethyl acetate with a small quantity of dichloromethane to afford 0.78 g of **2a** as a green solid. Yield 75%.

IR (KBr) ν_{max} 2930, 2855 (CH_2), 1590 (Ph), 745 cm^{-1} (S-CH_2).

The other $(C_nS)_8PcM$ ($n = 10$, 12, 16, $M = H_2$, Cu) derivatives were prepared in the same manner as described above. Table 2 summarizes the elemental analysis data and yields. The electronic absorption spectral data for all the phthalocyanine derivatives in this work are listed in Table 3. Each of the electronic absorption spectra showed Soret- and Q bands which are characteristic bands for phthalocyanine metal-free derivatives and copper complexes. For **1d** and **2d**, these longest chain-substituted compounds were poorly soluble and could not be completely dissolved in chloroform. Small amounts of undissolved powder could be seen in these solutions even at low concentrations. Hence, the absorption coefficients of these compounds could not be given in Table 3.

3 Results and discussion

3-1 Mesomorphism

3-1-1 Metal-free derivatives, $(C_nS)_8PcH_2$ ($n = 8$, 10, 12, 16). Table 4 lists the phase transition temperatures and enthalpy changes established by DSC and polarizing microscopic observations for the $(C_nS)_8PcH_2$ ($n = 8$, 10, 12, 16) derivatives (**1a** to **1d**). Each of the derivatives is crystalline at rt. When it was heated at 10 °C min^{-1}, it showed only a discotic hexagonal columnar (D_h) mesophase. On further heating, **1c** and **1d** cleared into an isotropic liquid (IL) at 281.6 °C and 228.4 °C, respectively, whereas the shorter-chain substituted derivatives, **1a** and **1b**, did not show clearing points till 400 °C but decomposed at *ca.* 340 °C.

1a has only one crystalline phase, whereas each of the other derivatives, **1b**, **1c** and **1d**, has crystalline polymorphs. Hence, their phase transition behaviors are quite complicated, as shown in Table 4. In Fig. 1a, all the mps and cps were plotted against the number of carbon atoms in the alkylthio chain. When a line was drawn through the higher mps, it showed a very smooth curve. Hence, the most stable crystalline phase may be found for each of the derivatives. As can be seen from this figure, they show a D_h mesophase over a wide temperature region.

These mesophases were identified by polarizing microscopic observations and X-ray diffraction measurements at 125 °C. The X-ray data were summarized in Table 5. The shorter-chain substituted derivatives, **1a** and **1b**, gave only one peak, in the low angle region and no natural texture, so that this mesophase could not be established. On the other hand, **1c** and **1d** gave two and three sharp peaks in the low angle region, respectively, so that each of the mesophases could be established as a discotic hexagonal columnar (D_h) mesophase. Hence, we deduced that each of the mesophases of **1a** and **1b** could be the same D_h phase as those of **1d** and **1c**. Fig. 2 shows a photomicrograph of the D_h mesophase of **1c** at 250 °C. For this typical fan-shaped texture often observed for D_h, this mesophase could be thus confirmed as a D_h phase.

3-1-2 Copper complexes, $(C_nS)_8PcCu$ ($n = 8$, 10, 12, 16). As can be seen from Table 4, each of the derivatives (**2a**–**2d**) shows

Table 3 UV–Visible spectral data of the $(C_nS)_8PcH_2$ ($n = 8$, 10, 12, 16) and $(C_nO)_8PcCu$ ($n = 8$, 10, 12, 16) derivatives

Compound	Concentration[a]/ 10^{-5} mol $^{-1}$	λ_{max}/nm (log ε)						
		Soret band			Q band			
1a: $(C_8S)_8PcH_2$	0.85	329.9(4.88)	359.1(4.84)	448.2(4.56)	636.7(4.55)	668.4(4.73)	700.2(5.14)	732.0(5.17)
1b: $(C_{10}S)_8PcH_2$	0.54	329.5(4.87)	359.1(4.84)	443.0(4.56)	634.8(4.54)	666.6(4.71)	700.4(5.14)	731.7(5.18)
1c: $(C_{12}S)_8PcH_2$	1.14	329.5(4.89)	359.3(4.85)	448.0(4.57)	636.8(4.56)	669.6(4.76)	699.6(5.14)	732.2(5.16)
1d: $(C_{16}S)_8PcH_2$	0.96[b]	329.0	359.3	449.5	636.1	667.7	699.4	731.3
2a: $(C_8S)_8PcCu$	1.09	264.3(4.73)	325.1(4.96)	440.0(4.53)	642.7(4.68)	*ca.* 680(sh)	711.3(5.20)	
2b: $(C_{10}S)_8PcCu$	0.85	264.0(4.680	324.1(4.94)	438.0(4.48)	642.4(4.66)	*ca.* 683(sh)	711.8(5.20)	
2c: $(C_{12}S)_8PcCu$	1.07	264.0(4.75)	324.9(4.97)	438.0(4.54)	642.6(4.69)	*ca.* 682(sh)	711.9(5.21)	
2d: $(C_{16}S)_8PcCu$[b]	1.02[b]	264.6	324.3	436.4	640.8	*ca.* 682(sh)	711.8	

[a]In chloroform. [b]These compounds were poorly soluble and did not dissolve completely in chloroform. Small amounts of powder remained undissolved even at this concentration. Hence, these absorption coefficients could not be given here.

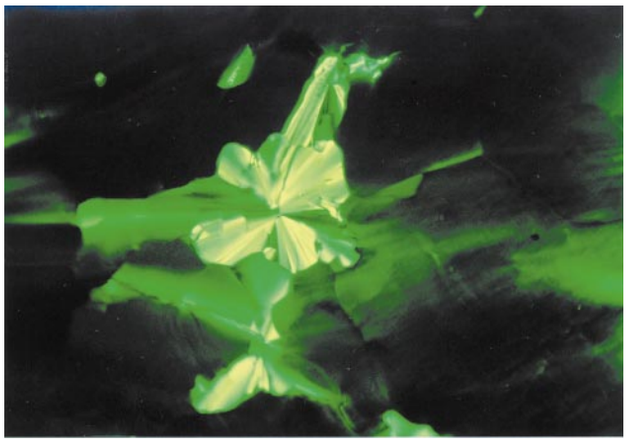

Fig. 2 Photomicrograph of the D_h mesophase of $(C_{12}S)_8PcH_2$ (**1c**) at 250 °C.

only one mesophase, D_h. The longer-chain substituted derivatives, **2c** and **2d** clear into isotropic liquid from the D_h mesophase at 322.8 °C and 261.7 °C, respectively. On the other hand, the shorter-chain substituted derivatives, **2a** and **2b**, give no isotropic liquid until 400 °C and decompose at *ca.* 290–350 °C, as do their metal-free derivatives.

The longer-chain substituted derivatives, **2c** and **2d**, showed crystalline polymorphs, as well as the metal-free derivatives. In Fig. 1b, all the phase transition temperatures were plotted against the number of carbon atoms in the alkylthio chain. When the highest mps were connected with a line, it showed a very smooth curve. Hence, the most stable crystalline phase could be found for each of the derivatives. Compared with the metal-free derivatives, they show a D_h mesophase at wider temperature region.

The mesophases were identified by microscopic observation and X-ray diffraction measurements at 125 °C. The X-ray data are listed in Table 6. Each of the copper complexes gave four to eight sharp peaks which spacings are in a ratio of $1:1/\sqrt{3}:1/2:1/\sqrt{7}\ldots$. Hence it could be identified as a D_h mesophase. Compared with the metal-free derivatives, these copper complexes gave higher-order reflections from the 2D-hexagonal lattice. This means that the copper complexes form more regularly packed columns than the metal-free derivatives. The lattice constants of the copper complexes are comparable to those of the metal-free derivatives (Tables 5 and 6).

Table 4 Phase transition temperatures and enthalpy changes of the $(C_nS)_8PcM$ (M = 2H, Cu, n = 8, 10, 12, 16) derivatives[a]

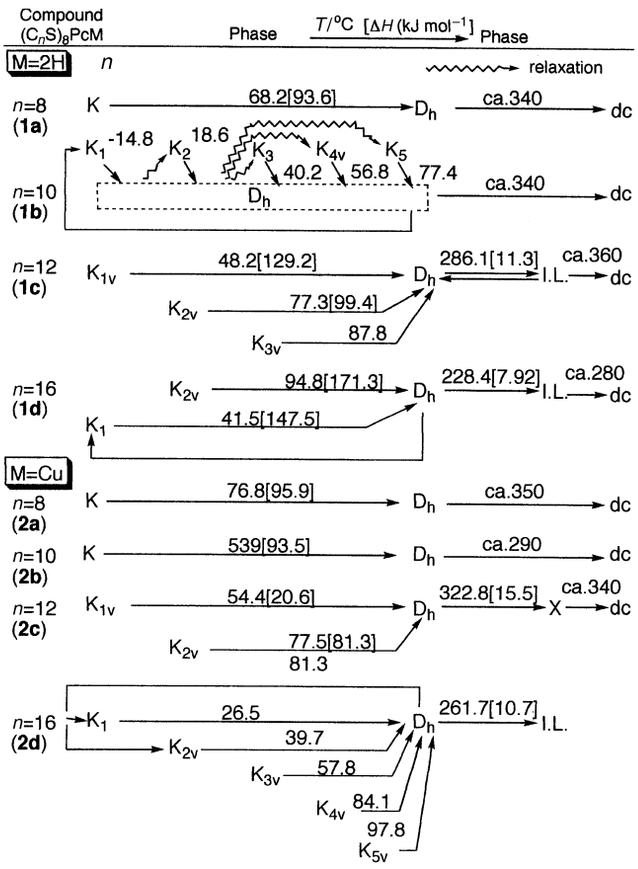

[a]Phase nomenclature: K = crystal, D_h = discotic hexagonal columnar mesophase, IL = isotropic liquid, dc = decomposition; X is an unidentified phase because of the limit of the instrument; v means virgin state (see Table 2). For each of the phases where no data are given the enthalpy change could not be accurately obtained, because the phase could not be obtained sufficiently pure for the determination.

3-1-3 Intracolumnar order. Fig. 3 illustrates the X-ray diffraction patterns of the metal-free derivatives, **1a** and **1d**, and the copper complexes, **2a** and **2d** at 125 °C.

Each of the patterns shows broad peaks at $2\theta \approx 13°$ (*ca.* 7 Å) and $2\theta \approx 25°$ (*ca.* 3.5 Å). When phthalocyanines form a columnar structure piled up face-to-face by the monomers, the stacking distance is generally 3.2–3.5 Å. For the dimers, it may be given the double value of 7 Å. Each of the present D_h mesophases gave both stacking distances (h_1 and h_2 in Fig. 3). This is attributable to a mixture of aggregated dimers and monomers in the columns.[1] Compared with the metal-free derivatives **1a** and **1d**, the longer-chain substituted one, **1d**,

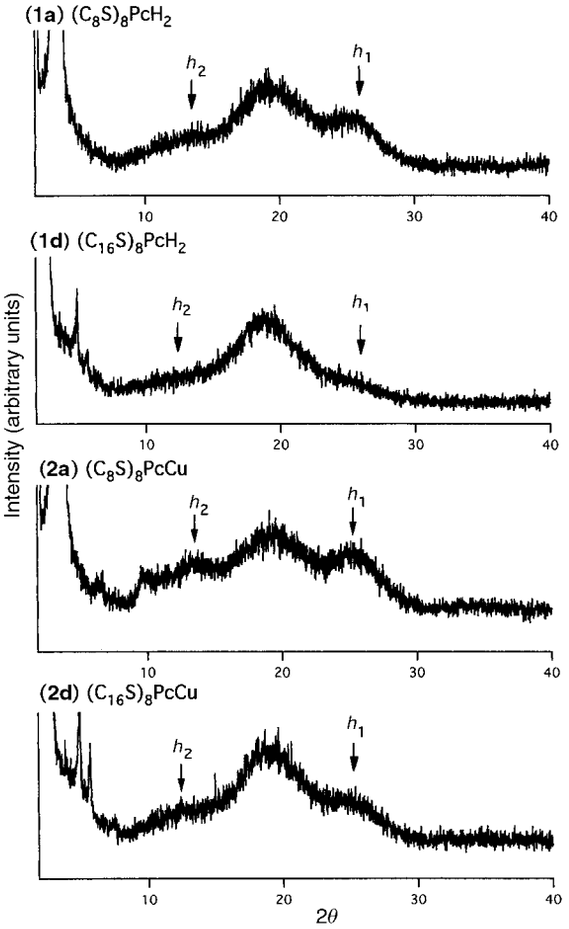

Fig. 3 X-Ray diffraction patterns of the $(C_8S)_8PcH_2$, $(C_{16}S)_8PcH_2$, $(C_8S)_8PcCu$ and $(C_{16}S)_8PcCu$ derivatives.

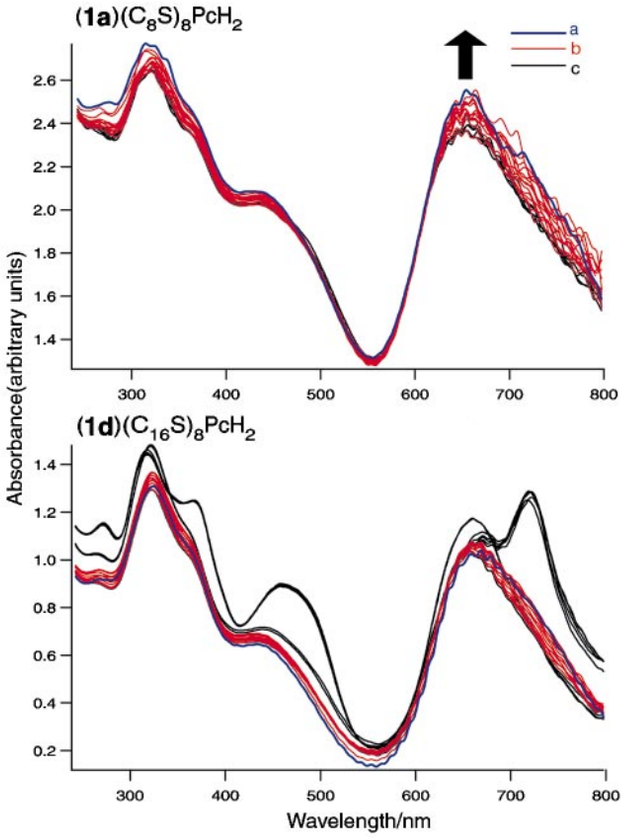

Fig. 4 Temperature-dependent electronic spectra of the UV–Vis region of the film of the $(C_8S)_8PcH_2$ and $(C_{16}S)_8PcH_2$ derivatives; a = spectrum of the isotropic liquid, b = spectra for the mesophase temperature region, c = spectra for the crystal temperature region.

gave smaller peaks h_1 and h_2. Comparing the copper complexes **2a** and **2d**, the same phenomenon can be seen. Hence, it can be deduced that the longer the peripheral chains become, the more the stacking distance between the central cores thermally fluctuates. Comparing the metal-free derivative and the copper complex with the same chain length, the copper complex has more ordered stacking than the metal free derivative.

To further clarify the molecular arrangement in the columns,

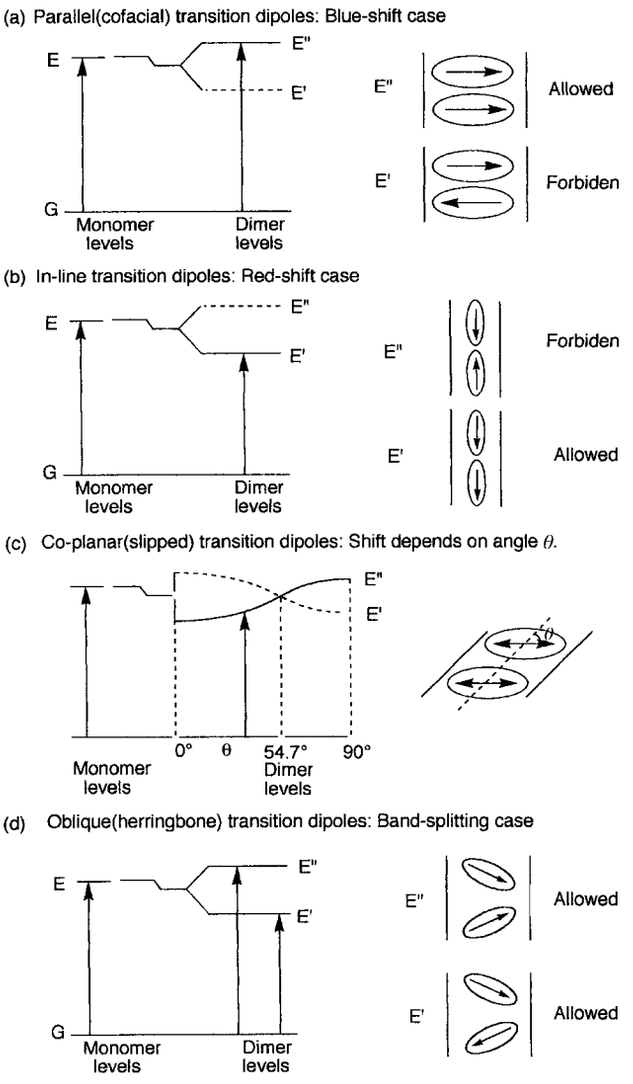

Fig. 5 Exciton energy diagrams for various dimers.

Table 5 X-Ray data of $(C_nS)_8PcH_2$ (n = 8, 10, 12, 16)

Compound (mesophase)	Lattice constant/Å	Spacing/Å		Miller indices (h k l)
		Observed	Calculated	
1a: $(C_8S)_8PcH_2$ (D_h at 125 °C)	a = 27.8	24.1	24.1	(1 0 0)
	h_2 = *ca.* 6.6	*ca.* 6.6	—	h_2[a]
	h_1 = *ca.* 3.5	*ca.* 4.6	—	$_b$
		ca. 3.5	—	h_1[a]
1b: $(C_{10}S)_8PcH_2$ (D_h at 125 °C)	a = 28.9	25.0	25.0	(1 0 0)
	h_2 = *ca.* 6.7	*ca.* 6.7	—	h_2
	h_1 = *ca.* 3.5	*ca.* 4.7	—	$_b$
		ca. 3.5	—	h_1
1c: $(C_{12}S)_8PcH_2$ (D_h at 125 °C)	a = 32.4	28.1	28.1	(1 0 0)
	h_2 = *ca.* 6.3	16.2	16.2	(1 1 0)
	h_1 = *ca.* 3.6	*ca.* 6.3	—	h_2
		ca. 4.6	—	$_b$
		ca. 3.6	—	h_1
1d: $(C_{16}S)_8PcH_2$ (D_h at 125 °C)	a = 36.1	31.2	31.2	(1 0 0)
	h_2 = *ca.* 6.4	18.1	18.1	(1 1 0)
	h_1 = *ca.* 3.5	15.6	15.6	(2 0 0)
		ca. 6.4	—	h_2
		ca. 4.7	—	$_b$

[a]h_2 = stacking distance between the dimers, h_1 = stacking distance between the monomers. [b]Halo of the molten alkylthio chains.

Table 6 X-Ray data of $(C_nS)_8PcCu$ ($n=8$, 10, 12, 16)

Compound (mesophase)	Lattice constant/Å	Spacing/Å		Miller indices (h k l)
		Observed	Calculated	
2a: $(C_8S)_8PcCu$ (D_h at 125 °C)	$a=28.0$	24.3	24.0	(1 0 0)
	$h_2=6.70$	14.0	13.9	(1 1 0)
	$h_1=ca.$ 3.5	12.1	12.0	(2 0 0)
		9.21	9.08	(2 1 0)
		8.20	8.09	(3 0 0)
		6.70	6.73	(1 3 0)+h_2[a]
		ca. 4.6	—	[b]
		ca. 3.5	—	h_1[a]
2b: $(C_{10}S)_8PcCu$ (D_h at 125 °C)	$a=29.9$	26.3	25.9	(1 0 0)
	$h_2=ca.$ 7.2	15.0	15.0	(1 1 0)
	$h_1=ca.$ 3.5	13.0	13.0	(2 0 0)
		9.86	9.80	(2 1 0)
		ca. 7.2	—	h_2
		ca. 4.7	—	[b]
		ca. 3.5	—	h_1
2c: $(C_{12}S)_8PcCu$ (D_h at 125 °C)	$a=32.2$	27.9	27.9	(1 0 0)
	$h_2=ca.$ 6.5	16.2	16.1	(1 1 0)
	$h_1=ca.$ 3.6	14.0	13.9	(2 0 0)
		10.6	10.5	(2 1 0)
		ca. 6.5	—	h_2
		ca. 4.6	—	[b]
		ca. 3.6	—	h_1
2d: $(C_{16}S)_8PcCu$ (D_h at 125 °C)	$a=35.8$	31.0	31.0	(1 0 0)
	$h_2=7.09$	18.0	17.9	(1 1 0)
	$h_1=ca.$ 3.5	15.6	15.6	(2 0 0)
		11.9	11.7	(2 1 0)
		8.98	8.96	(2 2 0)
		7.09	7.12	(2 3 0)+h_2
		5.92	5.97	(3 3 0)
		5.16	5.17	(0 6 0)
		ca. 4.6	—	[b]
		ca. 3.5	—	h_2

[a]h_2 = stacking distance between the dimers, h_1 = stacking distance between the monomers. [b]Halo of the molten alkylthio chains.

temperature-dependent electronic absorption spectra of casting films of **1a**, **2a**, **1d** and **2d** were measured at 10 °C intervals, as shown in Fig. 4 and 6. These spectra showed interference due to the thickness of the films at longer wavelength region.

Fig. 4 shows the spectra of the metal-free derivatives, **1a** and **1d**, from rt. to 210 °C. **1a** showed gradual increase of the absorbance with heating, but no big changes appeared. **1d** showed a broad Q band at rt., but for 40–80 °C, it showed a split Q band with higher intensities. This temperature region corresponds to the crystalline states (Table 4). Hence, in these crystalline phases the stacking of molecules is not parallel (face-to-face: Fig. 5(a)) but herringbone (Fig. 5(d)), from Kasha's rule.[12] Over this temperature range, the Q band for the D_h mesophase changed again into the previous non-split one similar to that for the crystals below 40 °C. On further heating, it showed no major changes.

Fig. 6 illustrates the spectra of the copper complexes, **2a** and **2d**, from rt. to 250 °C recorded at 10 °C intervals. **2a** showed a gradual increase of the absorbance with heating and at around 250 °C, a shoulder appeared on the Q band. This indicated that herringbone-shaped dimers tend to be formed at the higher temperatures. However, it did not give a clearly split Q band, so this tendency is not very great.

2d showed a split Q band in the crystalline temperature region, as well as **1d**. Over this temperature region, only a shoulder could be observed on the Q band. From these spectral changes it can be deduced that the molecules in columns form stacked herringbone-shaped dimers in the crystals, and on passing from crystal to mesophase it changes into parallel (face-to-face) dimer stacking: on further heating, the parallel dimer stacking gradually changes into herringbone-shape dimer stacking by thermal fluctuation.

Table 7 UV–Visible spectral data of the $(C_{12}S)_8PcM$, $(C_{12})_8PcM$, $(C_{12}O)_8PcM$ (M = 2H, Cu), and PcCu derivatives

Compound	Q band			
	λ_{max}/nm (log ε)			
$(C_{12}S)_8PcH_2$	636.8 (4.56)	669.6 (4.76)	699.6 (5.14)	732.2 (5.16)
$(C_{12})_8PcH_2$[a]	610 (—)	645 (—)	672 (—)	707 (5.0)
$(C_{12}O)_8PcH_2$[b]	600 (4.46)	640 (sh)	660 (5.19)	700 (5.23)
$(C_{12}S)_8PcCu$	642.6 (4.68)	*ca.* 680 (sh)	711.9 (5.21)	
$(C_{12})_8PcCu$[a]	618 (—)	657 (—)	687 (5.2)	
$(C_{12}O)_8PcCu$[b]	610 (4.77)	644–652 (sh)	675 (5.66)	
PcCu[c]	611 (4.56)	648 (4.51)	678 (5.34)	

[a]Ref. 5. [b]Ref. 4. [c]In 1-chloronaphthalene: ref. 13. In chloroform for the others.

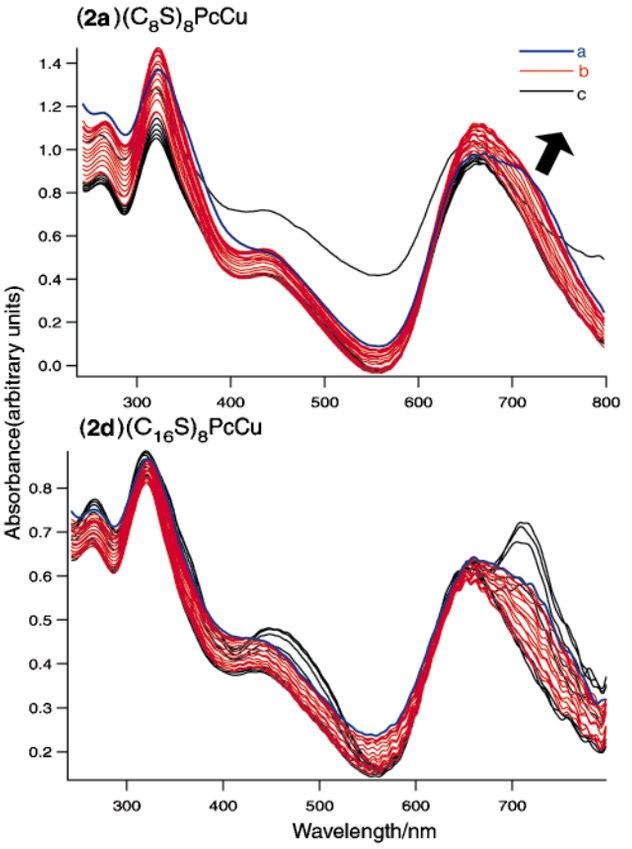

Fig. 6 Temperature-dependent electronic spectra of the UV–Vis region of the film of the $(C_8S)_8PcCu$ and $(C_{16}S)_8PcCu$ derivatives; a = spectrum of the isotropic liquid, b = spectra for the mesophase temperature region, c = spectra for the crystal temperature region.

3-2 Electroconductivity

According to the Hammett's σ_p values listed in Table 1, the Q bands of alkylthio-substituted phthalocyanines may shift to longer wavelength, compared with the Q bands of alkyl- and/or alkoxy-substituted phthalocyanines. The wavelengths of Q bands of the representative derivatives **1c** and **2c** are compared with the reported values for the octaalkylphthalocyanine[5] and octakis(alkoxy)phthalocyanine derivatives[4] ($(C_{12}X)_8PcM$, X = none, O; M = H_2, Cu). As can be seen from Table 7, the Q band of the dodecylthio-substituted derivatives largely shifts

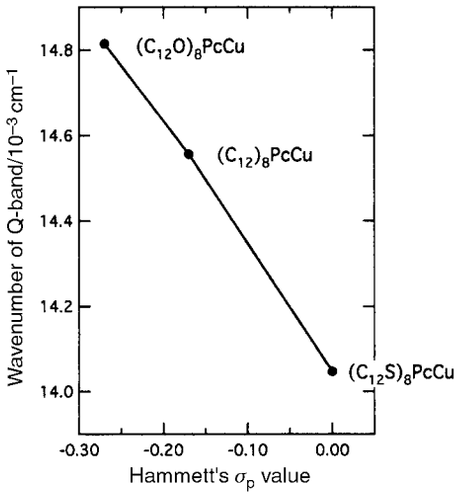

Fig. 7 The wave numbers of Q bands of these $(C_{12}X)_8PcM$ (X = S, none, O) complexes *versus* the Hammett's σ_p values of CH_3X (X = S, none, O).

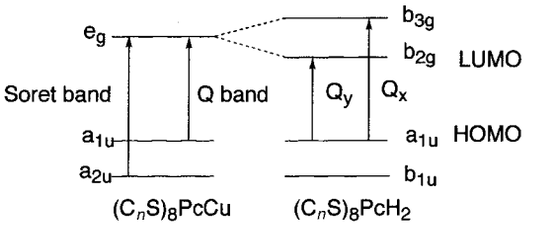

Fig. 8 Schematic energy levels of the Q bands of $(C_nS)_8PcM$ (M = 2H, Cu).

to longer wavelength, compared with the dodecyl-substituted and dodecyloxy-substituted ones. The wave numbers of Q bands of these $(C_{12}X)_8PcM$ (X = S, none, O) complexes were plotted against the Hammmett's σ_p values of CH_3X (X = S, none, O), in Fig. 7. This figure clearly shows a very good linearity between the wave numbers and σ_p values. However, the non-substituted copper complex, PcCu,[13] which corresponds to Hammett's $\sigma_p = 0$ for H in Table 1, is out of linearity (Table 7). Since we could not explain this only on the basis of the Hammett's σ_p values, something else may affect it. Further study is required.

As illustrated in Fig. 8, the Q bands correspond to the electronic transition between the HOMO and LUMO levels. Hence, the red-shift means that the energy gap between the HOMO and LUMO narrows on changing from alkyl and/or alkoxy groups to alkylthio groups. This may result in pushing up the electroconductivity, because electrons may more easily move in the one-dimensional columns giving a narrower energy gap. The electroconductivities were previously measured by using Pulse-Radiolysis Time-Resolved Microwave Conductivity (PR-TRMC) and it was shown that the conductivities of the alkylthio-substituted derivatives actually become higher than those of the alkoxy-substituted derivatives for the D_h mesophase: moreover, the $(C_{12}S)_8PcH_2$ derivative is the present record holder with a mobility value of 0.28 $cm^2\ V^{-1}\ s^{-1}$ (at 190 °C).[14]

4 Conclusion

Octakis(alkylthio)-substituted phthalocyanines (**1a** to **1d**) and their copper complexes (**2a** to **2d**) were synthesized. Each of the derivatives shows a D_h mesophase in very wide temperature region. In the D_h mesophases a mixture of monomer stacking and dimer stacking exists in the columns: with heating, the parallel dimer stacking gradually changes into herringbone-shape dimer stacking by thermal fluctuation. Comparing the mesophases of the metal-free derivatives and the copper complexes, more regularly packed columns and more ordered stacking in the columns could be seen for the copper complexes.

Acknowledgements

This work was partially supported by Grant-in-Aid for COE Research (10CE2003) by the Ministry of Education, Science, Sports and Culture of Japan.

References

1 Part 26: K. Ohta, S. Azumane, N. Kobayashi and I. Yamamoto, *J. Mater. Chem.*, 1999, **9**, 2313.
2 N. Ishikawa and Y. Kaizu, *Nippon Kagaku Kaishi*, 1997, **10**, 633.
3 P. G. Schouten, J. M. Warman, M. P. de Haas, C. F. van Nostrum, G. H. Gelinck, R. J. M. Nolte, M. J. Copyn, J. W. Zwikker, M. K. Engel, M. Hanack, Y. H. Chan and W. T. Ford, *J. Am. Chem. Soc.*, 1994, **116**, 6880.
4 R. J. Nolte and W. Drenth, *Recl. Trav. Chim. Pays-Bas*, 1988, **107**, 615.
5 H. Nishi and S. Ueno, *Nippon Kagaku Kaishi*, 1989, 983.

6 D. Adam, P. Schuhmacher, J. Simmerer, L. Häissling, K. Siemensmeyer, K. H. Etzbach, H. Ringsdorf and D. Haarer, *Nature*, 1994, **371**, 141.
7 H. Eichhorn and D. Wöhrle, *Liq. Cryst.*, 1997, **22**, 643.
8 H. Ema, Master's Thesis, Shinshu University, Ueda, 1988, ch. 7.
9 H. Hasebe, Master's Thesis, Shinshu University, Ueda, 1991, ch. 5.
10 Y. Suda, K. Shigehara, A. Yamada, H. Matuda, S. Okada, A. Masaki and H. Nakanishi, *SPIE*, 1991, **1560**, 75.
11 D. Wöhrle, M. Eskers, K. Shigehara and A. Yamada, *Synthesis*, 1993, 194.
12 M. Kasha, H. R. Rawls and M. Ashraf El-Bayoumi, *Pure Appl. Chem.*, 1965, **11**, 371.
13 E. A. Cuellar and T. J. Marks, *Inorg. Chem.*, 1981, **20**, 3766.
14 A. M. van de Craats, P. G. Shouten and J. M. Warman, *Ekisho*, 1998, **2**, 12.
15 N. Inamoto, *Hametto Soku—Kozo to Hannousei*, ("Hammett's Rule—Structures and Reactivities"), Maruzen, 1983, p. 143.